Pergamon

Int. J. Heat Mass Transfer. Vol. 38, No. 16, pp. 2969–2984, 1995

0017-9310/95 $9.50+0.00

0017-9310(95)00039-9

A numerical investigation of conjugate heat transfer from a flush heat source on a conductive board in laminar channel flow

RAMESH SUGAVANAM† and ALFONSO ORTEGA
Department of Aerospace and Mechanical Engineering, The University of Arizona, Tucson, AZ 85721, U.S.A.

and

C. Y. CHOI‡

Department of Agricultural and Biosystems Engineering, The University of Arizona, Tucson, AZ 85721, U.S.A.

(*Received* 25 *September* 1994 *and in final form* 18 *January* 1995)

Abstract—A numerical investigation was conducted on the heat transfer from a uniformly powered strip source of heat located on the surface of a two-dimensional conducting substrate. The upper and lower surfaces of the substrate are cooled by forced laminar flow that is two-dimensional, steady and with constant properties. The problem is a paradigm for the investigation of the competing effects of substrate conduction and fluid convection in the cooling of electronic components, i.e. chips or chip carriers, on boards or substrates that are cooled by air flowing parallel to the surface. The objectives of the study were to investigate the conjugate heat transfer mechanisms in great detail and in a methodical way, such as to use the results as a baseline for successively more complex situations of air-cooling of on-board components. Results are presented for the substrate conductivity to fluid conductivity ratio, k_s/k_f from 0.1 to 100, channel Reynolds number from order 100 to order 1000, corresponding to air velocities of order 1 m s^{-1}, and for both developing and fully developed laminar, parallel-plane channel flow.

INTRODUCTION

The thermal design of air-cooled packaging has at least three distinct hierarchies, the chip and package level, the board level and the cabinet or enclosure level. The present paper addresses the mid-level problem, that is, the thermal phenomena at the board level. What is the board-level problem? In essence it may be distilled to a relatively straightforward objective which is "to predict the chip junction temperature internal to a component, parametric on position on the board, parametric on component internal thermal resistance, parametric on component-to-board thermal coupling, parametric on board thermal characteristics such as thickness, conductivity, and density of metallization layers, parametric on the local convective environment, and parametric on the thermal interactions with neighboring components." Before board layout and routing can be completed, the design must satisfy thermal constraints on maximum operating temperature in the face of all of the above parameters. Indeed this becomes a complex design process necessitating a suite of modeling and simulation tools for all three hierarchical levels and for combined electrical, thermal and mechanical phenomena. Many such tools have been developed in recent years, and promising advances have been made in the development of concurrent design and simulation environments that begin with MCAD and ECAD tools and end with simulation, for example the simulation of the thermal field on a package on a populated board subjected to an air-cooled convective environment, or the simulation of the signal propagation and delay in a specific electrical interconnection.

The present work addresses a specific sub-issue related to the thermal behavior, and the simulation thereof, of an air-cooled component on a conducting board. The issue is that in any air-cooled situation, the heat transfer from a power dissipating component to the air involves a direct path to the air, and an indirect path through the board to the air. Because of the discrete nature of the heat source on the board, the thermal boundary conditions on the board are highly non-uniform and therefore make the use of a surface specified conductance, i.e. a heat transfer coefficient, difficult if not impossible. In traditional

†Present address: Automated Analysis Corporation, 423 SW Washington, Peoria, IL 61614, U.S.A.
‡Author to whom correspondence should be addressed.

NOMENCLATURE

D_h	hydraulic diameter, $2H$ for parallel plates [m]
H	channel height [m]
k_s/k_f	ratio of thermal conductivity of the substrate to that of the fluid
L	length of channel [m]
L_d	distance between sources [m]
L_s	source length [m]
N	number of iteration
Nu	Nusselt number, equation (18)
Nu_s	average Nusselt number on the source, equation (19)
p	pressure [Pa]
P	$p/\rho U_0^2$ non-dimensional pressure
Pe	$RePr$, Peclet number
Pr	Prandtl number
q	source heat flux [W m^{-2}]
q_f	heat flux from the board into the fluid [W m^{-2}]
Ra	Rayleigh number
Re	$U_0 D_h/\nu$, Reynolds number
T	temperature [°C]
T_0	inlet temperature [°C]
t	thickness of the substrate [m]
u	streamwise velocity [m s^{-1}]
U_0	inlet velocity [m s^{-1}]
U	u/U_0 non-dimensional streamwise velocity
v	transverse velocity [m s^{-1}]
V	v/U_0 non-dimensional transverse velocity
x	channel streamwise coordinate [m]
x_s	location of the source from the inlet on the interface [m]
X	x/D_h non-dimensional channel streamwise coordinate
X_s	x_s/D_h non-dimensional location of the source from the inlet on the interface
y	channel transverse coordinate [m]
Y	y/D_h non-dimensional channel transverse coordinate.

Greek symbols

α	thermal diffusivity [m^2 s^{-1}]
θ	dimensionless temperature
ν	kinematic viscosity [m^2 s^{-1}]
ρ	density [kg m^{-3}].

Subscripts

b	back
f	front
fm	thermally fully developed mixed mean
i	interface
m	mixed mean
max	maximum
s	source
0	at channel inlet.

technologies that make use of internal forced convection heat transfer, notably compact heat exchangers, the use of a constant surface conductance that is derived by assuming that the thermal boundary conditions are uniform, be they temperature or heat flux, is successful because the surface conductance is well behaved. In air-cooling of electronics, the use of a surface conductance as a boundary condition for a package-level conduction analysis is a way of uncoupling the board-level phenomena from the package internal thermal phenomena. However, the local surface conductance is highly dependent on the nature of the thermal boundary conditions upstream and in the vicinity of the package. In the face of highly non-uniform surface temperature and heat flux on the surface of a board, the local surface heat transfer coefficient is highly non-uniform, especially if defined in terms of a fixed reference temperature such as channel inlet temperature. In air-cooling of electronics, the fact that the power is dissipated from discrete spatial areas and the fact that the board conduction assists in the 'heat spreading' make the surface temperature and heat flux highly non-uniform on the surface of a board populated with components.

The present numerical study involves the simplest geometry that can be used as a paradigm for investigating coupled conduction–convection mechanisms. The physical geometry is shown in Fig. 1. Its essential features are that the heating occurs from a dicretized source and the substrate is conducting. The heat generated in the components can be directly dissipated from the exposed surface by convection or indirectly by conduction through the board first and then by convection to the air stream. In the actual situation, various complexities are involved, including complex flow in a laminar, transitional, or low Reynolds number turbulent regime, elevated levels of turbulence in the flow, package-level conduction and package to board thermal coupling. The goals of the study are twofold: (1) to establish the thermal behavior for the conjugate conduction–convection problem as a computational benchmark for successively more complex geometries that are presently being studied; and (2) to use the results of the numerical investigation to assess the possibility of using more approximate approaches, using the surface heat transfer coefficient approach. In the context of these goals, one of our primary objectives, therefore, is to perform a

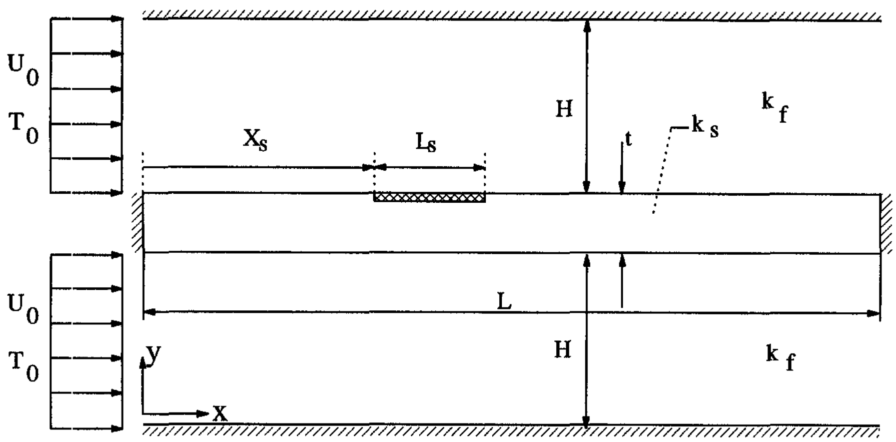

Fig. 1. Schematic for the conjugate problem with a discrete flush-mounted source.

thorough parametric evaluation of the effects of board conduction on the overall heat transfer.

PREVIOUS STUDIES

The previous work done in the field of forced convection conjugate heat transfer for laminar flow conditions is discussed in Peterson and Ortega [1]. Baker [2] conducted an analytical and experimental investigation of cooling of microelectronic devices by free and forced convection. His study included small isothermal heat sources mounted on an insulated board in a turbulent boundary layer with uniform properties and a universal velocity profile using freon 113 as the coolant. Brosh *et al.* [3] numerically solved the problem of a two-dimensional laminar incompressible flow over a conducting plate with a line heat source (a point source in the two-dimensional sense) located at the solid–fluid interface perpendicular to the flow direction. An investigation into the conjugate analysis of forced convection heat transfer from small isothermal heat sources embedded in a large substrate for hydrodynamically fully developed laminar channel flow was performed by Ramadhyani *et al.* [4]. Incropera *et al.* [5] studied the problem of flush mounted isothermal heat sources embedded in one wall of the horizontal channel with hydrodynamically fully developed laminar or turbulent flow. They conducted both experimental and theoretical studies of this problem. They compared their numerical investigations with data from single square sources and an array of 12 such sources in water and FC77. They concentrated their effort on understanding the behavior of the surface conductance on the surface of the heat source. Culham *et al.* [6, 7] conducted a study of conjugate heat transfer from square flush mounted heat sources by implementing an iterative scheme in which the thermal boundary conditions are applied on the conduction solution based upon the analytical solution of the boundary-layer energy equation. Davalath and Bayazitoglu [8] considered the effects of conduction to the board onto which three repeating, heated rectangular components were attached, and analysed two-dimensional conjugate heat transfer in the entrance region for this geometry. In increasing the board-to-fluid thermal conductivity ratio from 1 to 10, the Nusselt number over the component was found to be affected significantly. Kim and Anand [9, 10] conducted a numerical investigation based on the finite volume method to analyse two-dimensional laminar and turbulent heat transfer between a series of parallel plates with surface-mounted discrete block heat sources. They found that the overall thermal resistance of the module reduced with increasing substrate conduction effects and increasing Reynolds number. They also demonstrated that substrate conduction is an important parameter in the design and analysis of cooling channels of electronic equipment. Choi *et al.* [11] studied the effects of substrate conductivity in the cooling of electronic components mounted on a PCB. They conducted a numerical investigation for two cases: a single heat-dissipating component and five heat-dissipating components. They observed that the local Nusselt number was the highest for the first module and then decreased for subsequent modules. They found that the Nusselt number varied periodically with a decreasing mean and this variation gradually disappeared with increasing conductivity ratios. They also demonstrated that the maximum temperature within the modules could be greatly reduced by increasing the PCB conductivity. Nigen and Amon [12] studied forced convective heat exchangers consisting of multimaterial solid domains with concentrated heat generation. They found that concentrated heat generation (conjugate conduction–convection simulations) exhibited different thermal performance from uniform heat flux representations (convection-only simulations). They also demonstrated the significance of considering time-dependent flow characteristics.

The present work was conducted concurrently with equally detailed experimental work on the same geometry (Ortega *et al.* [13]). In both studies, it was found that a thorough documentation of the heat transfer from the source, the thermal wake effects, and the upwind conduction effects was not available through the entire regime of developing to fully developed flow conditions. In summary, the principal objective of the work was to perform detailed analysis on this paradigm to gauge the suitability of using simpler uncoupled models for air-cooled electronics.

ANALYSIS

The domain of interest is a two-dimensional parallel-plate channel with a conductive wall where a one-dimensional (i.e. an infinite strip) flush heat source is deployed. The other wall is insulated. We consider two-dimensional laminar flow in the channel with a uniform inlet velocity profile. The exit conditions are that the streamwise velocity and temperature gradients in the flow direction vanish at the exit plane. To examine the effect of the back-side boundary conditions, two cases, (i) insulated back-side and (ii) convectively cooled back-side, were examined. To conduct the study for fully developed flow and slug flow cases, the velocity distribution was imposed *a priori* so that only the energy equation was solved numerically. The mathematical formulation for the first case of an insulated back-side is presented in the following.

GOVERNING EQUATIONS

The flow field is assumed to be steady, two-dimensional, Newtonian, incompressible and laminar. The properties of the material of the substrate and the fluid are considered to be uniform, isotropic and constant. The non-dimensional variables of the governing equations are given by

$$X=\frac{x}{D_h} \quad Y=\frac{y}{D_h} \quad U=\frac{u}{U_0}$$

$$V=\frac{v}{U_0} \quad \theta=\frac{T-T_0}{q''D_h/k_f} \quad P=\frac{p}{\rho U_0^2} \tag{1}$$

$$Re=\frac{U_0 D_h}{\nu} \quad Pr=\frac{\nu}{\alpha} \quad Pe=Re\,Pr. \tag{2}$$

The governing equations for the fluid side are:

continuity

$$\frac{\partial U}{\partial X}+\frac{\partial V}{\partial Y}=0 \tag{3}$$

X-momentum

$$U\frac{\partial U}{\partial X}+V\frac{\partial U}{\partial Y}=-\frac{\partial P}{\partial X}+\frac{1}{Re}\left[\frac{\partial^2 U}{\partial X^2}+\frac{\partial^2 U}{\partial Y^2}\right] \tag{4}$$

Y-momentum

$$U\frac{\partial V}{\partial X}+V\frac{\partial V}{\partial Y}=-\frac{\partial P}{\partial Y}+\frac{1}{Re}\left[\frac{\partial^2 V}{\partial X^2}+\frac{\partial^2 V}{\partial Y^2}\right] \tag{5}$$

energy

$$U\frac{\partial \theta}{\partial X}+V\frac{\partial \theta}{\partial Y}=\frac{1}{Pe}\left[\frac{\partial^2 \theta}{\partial X^2}+\frac{\partial^2 \theta}{\partial Y^2}\right] \tag{6}$$

and the corresponding dimensionless boundary conditions at the inlet and exit are

$$U=1\ V=0, \theta=0 \quad \text{for } X=0 \quad \text{and } \frac{t}{D_h}\leqslant Y\leqslant\frac{H+t}{D_h} \tag{7}$$

$$\frac{\partial U}{\partial X}=0, V=0, \frac{\partial \theta}{\partial X}=0 \quad \text{for } X=\frac{L}{D_h} \quad \text{and } \frac{t}{D_h}<Y<\frac{H+t}{D_h}. \tag{8}$$

The no-slip conditions at the interface and top wall are formulated as

$$U=0, V=0 \quad \text{for } 0\leqslant X\leqslant L/D_h \quad \text{and } Y=\frac{t}{D_h}, Y=\frac{H+t}{D_h} \tag{9}$$

and the insulated top wall condition is given as

$$\frac{\partial \theta}{\partial Y}=0 \quad \text{for } 0\leqslant X\leqslant\frac{L}{D_h}, \text{ and } Y=\frac{H+t}{D_h}. \tag{10}$$

The energy equation on the solid side is posed as

$$\frac{\partial^2 \theta}{\partial X^2}+\frac{\partial^2 \theta}{\partial Y^2}=0. \tag{11}$$

The ends of the substrate are taken to be insulated, implying:

$$\frac{\partial \theta}{\partial X}=0 \quad \text{for } X=0, X=\frac{L}{D_h} \text{ and } 0\leqslant Y\leqslant\frac{t}{D_h} \tag{12}$$

$$\frac{\partial \theta}{\partial Y}=0 \quad \text{for } 0\leqslant X\leqslant\frac{L}{D_h} \text{ and } Y=0. \tag{13}$$

The non-dimensional matching interface conditions are stated by the matching heat flux and the matching temperature:

$$\frac{k_s}{k_f}\left(\frac{\partial \theta}{\partial Y}\right)_s=\left(\frac{\partial \theta}{\partial Y}\right)_f \quad \text{for } 0\leqslant X\leqslant X_s \quad \text{and } X_s+\frac{L_s}{D_h}\leqslant X\leqslant\frac{L}{D_h} \tag{14}$$

$$\frac{k_s}{k_f}\left[\frac{\partial \theta}{\partial Y}\right]_s-\left[\frac{\partial \theta}{\partial Y}\right]_f=1 \quad \text{for } X_s\leqslant X\leqslant X_s+\frac{L_s}{D_h} \tag{15}$$

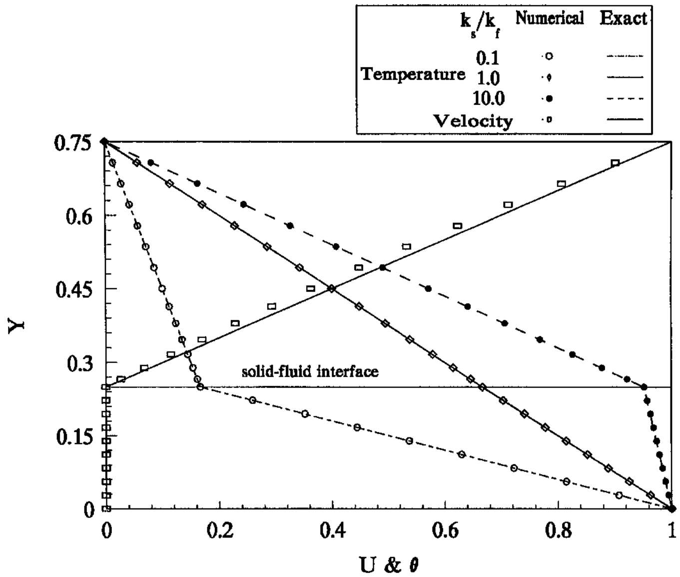

Fig. 2. Comparison of conjugate benchmark solution for Couette flow conditions.

$$\theta_f = \theta_s \quad \text{for } 0 \leqslant X \leqslant \frac{L}{D_h} \text{ and } Y = \frac{t}{D_h}. \quad (16)$$

The formulation remains the same for the case of a convectively cooled back-side with the exception of the back-side boundary conditions. The domain on the back-side is the same as that on the front-side of the board, except that there is no heat source on the back-side. The full two-dimensional momentum and energy equations are solved on the back-side with the matching interface conditions.

A numerical solution is sought for the set of equations derived above using the well-documented SIMPLER scheme described by Patankar [14]. The detailed procedure for the discretization with the convective and diffusive terms is in the thesis of Sugavanam [15]. To qualify the code, the code was validated by solving the benchmark problem of natural convection in a square enclosure and results were compared with those presented by de Vahl Davis and Jones [16]. The comparison showed that the overall Nusselt numbers were within 2% of the benchmark solution for Rayleigh numbers in the range 10^3–10^6. The code was also validated against a conjugate Couette flow problem in a parallel plate channel where one of the walls moves at a constant velocity and the other wall is a stationary conducting solid. The outer surface of the conducting solid is maintained at a constant temperature that is higher than the constant temperature of the opposing channel wall. The inlet and the exit streamwise velocity and temperature gradients were taken as zero while the normal velocity component is neglected. An analytical solution is available for the problem, for example as shown in White [17]. As shown in Fig. 2, the computational results demonstrate excellent agreement with the analytical solution for varying conductivity ratios. The velocities compared within 2% while the temperatures compared within 0.5% of the anaytical solution. Note that the fluid/solid interface is located at $Y = 0.25$ in Fig. 2.

The convergence criteria was defined as

$$|\Phi^{N+1} - \Phi^N| < 10^{-4} \quad (17)$$

where N and Φ represent the number of iterations and the dependent variables, V, U and θ respectively. No significant improvement in maximum temperature and Nusselt number was observed for tighter convergence. A number of grid tests were conducted varying with the mesh sizes in order to select an appropriate mesh size. A staggered, non-uniform mesh 51 in the normal and 277 in the streamwise direction was selected for the present calculations. The energy balance check, neglecting the axial conduction in the fluid at the entrance, had a maximum error of 2%. Computations were performed on the CONVEX 240.

Because of the elliptic nature of the conjugate problem, it was necessary to inquire whether the artificial exit boundary conditions given by equation (8) of parallel flow and vanishing streamwise temperature gradients did not artificially constrain the solution, especially in the vicinity of the source. The development of thermally fully developed conditions is dependent on the Peclet number. For the present problem, when the average velocity of air is 1 m s^{-1} at the inlet, the Peclet number is 882. This Peclet number necessitates a very long channel to achieve thermally fully developed conditions at the exit. Tests were performed by varying the channel length to study the infuence of the exit boundary condition on the heat transfer characteristics in the domain. From the overall energy balance for a long channel, the fully developed mixed mean temperature is derived as

Table 1. Effect of exit boundary conditions on maximum source temperature and source averaged Nusselt number for insulated back-side and $Pe = 882$

k_s/k_f	L/D_h	θ_{max}/θ_{fm}	$\overline{Nu_s}$
	8	48.88132	25.49818
0.1	10.5	48.88436	25.49736
	13	48.88541	25.49709
	8	30.45855	1900939
10.0	10.5	30.45829	19.00803
	13	30.45810	19.00700

Table 2. Effect of exit boundary conditions on maximum source temperature and source averaged Nusselt number for convectively cooled back-side and $Pe = 882$

k_s/k_f	L/D_h	θ_{max}/θ_{jm}	$\overline{Nu_s}$
	8	96.38974	25.55326
0.1	10.5	96.39616	25.55244
	13	96.39838	25.55216
	8	43.04848	20.46753
10.0	10.5	43.04706	20.46598
	13	43.04674	20.46545

$$\theta_{fm} = \frac{1}{Pe}.$$

The length of the channel from the source to the exit was varied from 10 to 20 cm. Table 1 indicates that there was no appreciable difference in the maximum temperature and the average Nusselt number on the source, hence the majority of the calculations were performed with $L/D_h = 8$. In none of the cases is the flow thermally fully-developed. For the case of a convectively cooled back-side, the fully developed mixed mean temperature is given by:

$$\theta_{fm} = \frac{1}{2Pe}.$$

This mixed mean temperature is achieved at the exit for a very long channel at all conductivity ratios, and the fluid on both sides of the substrate and the substrate itself equilibrate to this value. In other words, the fully-developed temperature profile is a uniform temperature throughout the exit plane. The effects of overall channel length, with the exit conditions specified by equation (8), on the local source maximum temperature and Nusselt number are given in Table 2. Again, $L/D_h = 8$ was found to be satisfactory for all cases.

RESULTS AND DISCUSSION

The critical features of this problem are that the heating occurs from a discretized heat source and that the board is conducting. A comprehensive parametric study was conducted to show the variation of interface temperature and the Nusselt number with the conductivity ratio, source location, Reynolds number and substrate thickness for the flow conditions varying from slug flow to fully developed flow. Results are discussed in two sections: (i) insulated back-side of the board and (ii) convectively cooled back-side of the board.

Back-side insulated

For most of this study, the Reynolds number was maintained constant at a value corresponding to 1.0 m s^{-1} average inlet velocity in a parallel-plate channel of height 1 cm. Ortega *et al.* [13] have demonstrated that air velocities of 1 m s^{-1} produce subcritical flow, and transition to turbulence is highly dependent on geometric disturbances, such as those commonly encountered on PCBs, for velocities higher than 2 m s^{-1}. Thus a velocity of 1 m s^{-1} is safely laminar, as observed experimentally. The heat source streamwise length was chosen as 1 cm and the substrate thickness was taken as 0.5 cm. The location of the source in the channel was variable. Variations of temperature, heat flux into the fluid and Nusselt number along the interface, for a fully developed flow maintained at a constant Reynolds number and k_s/k_f varying between 0.1 and 100 are shown in Figs. 3–6. In these figures, the source is located at a position $2.5 \leqslant X \leqslant 3.0$. The interface temperature profiles are shown in Fig. 3. Figure 3 clearly demonstrates the spreading of the temperature profiles and the decreasing maximum temperature for higher substrate conductivities. The normalized temperature along the interface remains undisturbed until the upstream conduction becomes non-negligible. It then rises until it reaches a maximum on the heat source and decreases thereafter. In the wake region downstream of the source, the non-dimensional temperatures for all conductivity ratios merge. It is especially instructive to learn that the downstream thermal wake achieves the adiabatic board behavior within only one lengthscale downstream, for $k_s/k_f \leqslant 10$, and within two length scales for greater conductivities. The use of thermal wake solutions derived for non-conducting (adiabatic) boards has been proposed by Ortega *et al.* [18] and Ramanathan and Ortega [19], and their use is justified by present results. This is partly explained by the variation of the heat flux into the fluid side shown in Fig. 4. For increasing k_s/k_f the spreading of the heat flux because of the board conduction is readily apparent, but we note that the conduction is preferentially to the upstream surface since the near-wall fluid is cooler in this region. From Fig. 4, it can be observed that far downstream there is no heat flux into the fluid from the board. Since the board is insulated on all the sides except for the side that is open to the fluid flow, the total heat from the source must be dissipated into the fluid either by convection directly from the source or by conduction through the board first and then by convection into the air stream. Hence, in the far downstream wake region, the upstream distribution of the heat flux from the board into the fluid caused

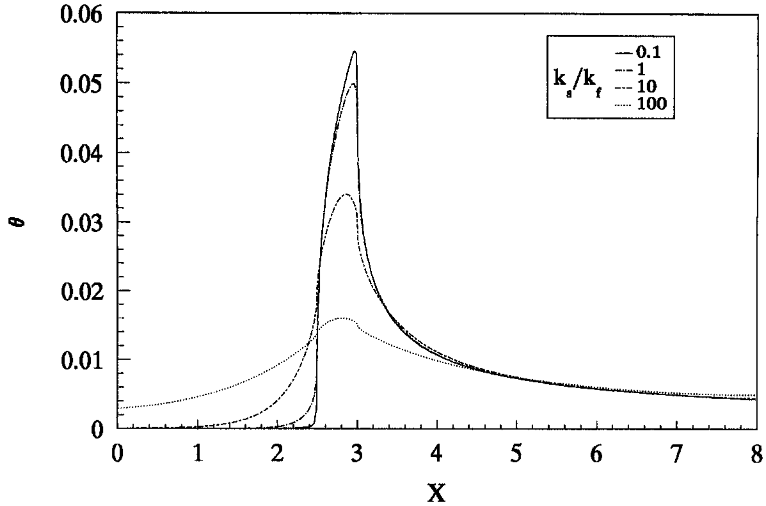

Fig. 3. Interface temperature varying with position for fully developed flow at Re = 1260.0 for the case of insulated back-side of the board.

by board conduction has little effect on the wall temperature, remaining the same as it does for all k_s/k_f ratios, for fixed total heat input into the fluid from the board.

Figure 5 shows the variation of the Nusselt number, based on the inlet temperature as the reference, along the interface. The Nusselt number is defined as

$$Nu = -\left(\frac{1}{\theta_f}\frac{\partial \theta_f}{\partial Y}\right)_i. \quad (18)$$

The Nusselt number over the source decreases in the downstream direction on the source, and rapidly approaches zero thereafter. In the downstream wake region the heat flux approaches zero but, because of the convective wake effect, the interface temperature elevation over the inlet temperature does not, thus Nu approaches zero. The Nusselt number in the upstream region is a ratio of two small numbers, the heat flux from the board into the fluid and the temperature rise of the interface over the inlet. In the upstream region the ratio is nearly constant, but its value is dependent on the conductivity ratio. Nu is lowest for the most conductive case. This is caused by the highest board conductivity inducing the greatest tendency for heating of the near-wall fluid upstream of the source. The Nusselt number shows a sharp increase near the beginning of the source for low board conductivities. With increase in the substrate conductivity the gradient at the leading edge of the source decreases. It is clear that because of the non-uniformity in both the surface temperature and flux, the surface conductance or heat transfer coefficient, h, varies greatly and is a strong

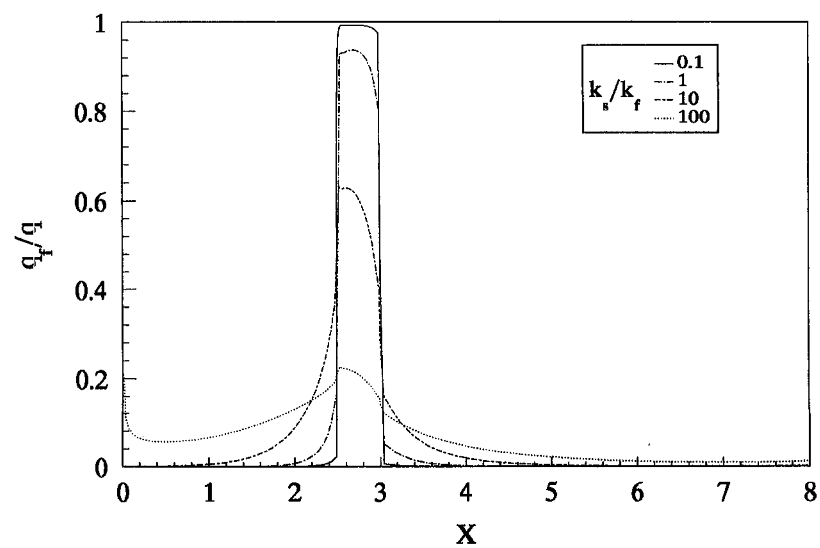

Fig. 4. Heat flux into the fluid varying with position for fully developed flow at Re = 1260.0 for the case of insulated back-side of the board.

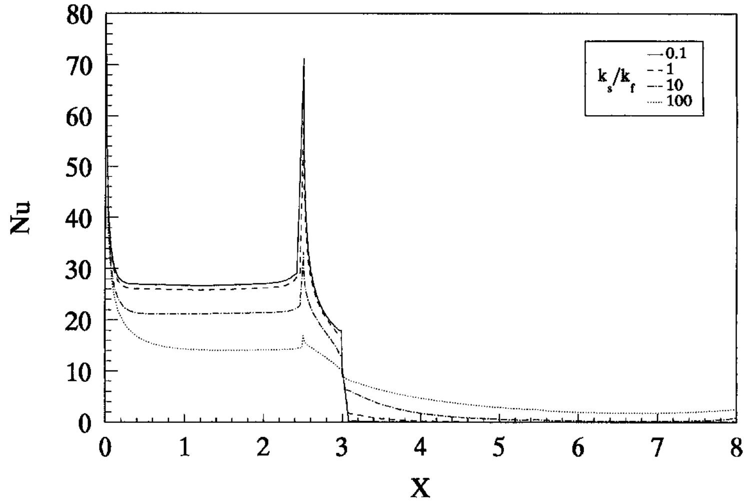

Fig. 5. Nusselt number on the interface varying with position for fully developed flow at $Re = 1260.0$ for the case of insulated back-side of the board.

function of the substrate conductivity. Figure 6 shows the spatial dependence of Nu on the heat source itself. The fact that Nu decreases for increasing conductivity is merely a reflection of the preheating of the near-wall fluid due to the upstream conduction. The difference in the behavior of Nu in the upstream region of the source compared with the downstream region is an excellent example of the difficulty in predicting Nu in heat transfer problems that have significant conjugate coupling and highly non-uniform surface thermal boundary conditions. As also noted by Zebib and Wo [20], it is impossible to specify the surface conductance or the reference temperature *a priori* because of the conjugate coupling. The substrate conduction obviously has an elliptic character that prevents the determination of the fluid-side temperature field and the surface conductance by marching the solution of the energy equation in the streamwise direction, as, for example, in an integral solution to the boundary-layer problem. Figure 7 demonstrates the previous statement in a very practical way. Here, the average Nusselt number on the source, referenced to the inlet temperature, is shown as a function of k_s/k_f for a Reynolds number corresponding to 1 and 0.1 m s^{-1} inlet air velocity respectively. The flow is fully developed in all cases. The average Nusselt number on the source is defined as

$$\overline{Nu_s} = \frac{1}{L_s/D_h}\int_{X_s}^{X_s+(L_s/D_h)} Nu\,\mathrm{d}X. \tag{19}$$

In any practical thermal design tool that does not explicitly solve the full conjugate problem, the prediction of junction temperature is most likely to be performed with a conduction solver using an uncoupled approach, i.e. an approach in which the surface conductance is specified as a boundary condition on the package surfaces. More than likely, the

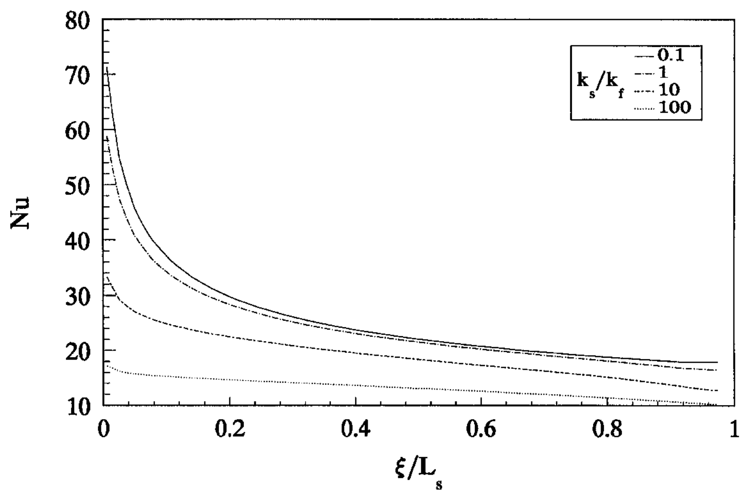

Fig. 6. Nusselt number on the heat source as a function of position for fully developed flow at $Re = 1260.0$ for the case of insulated back-side of the board.

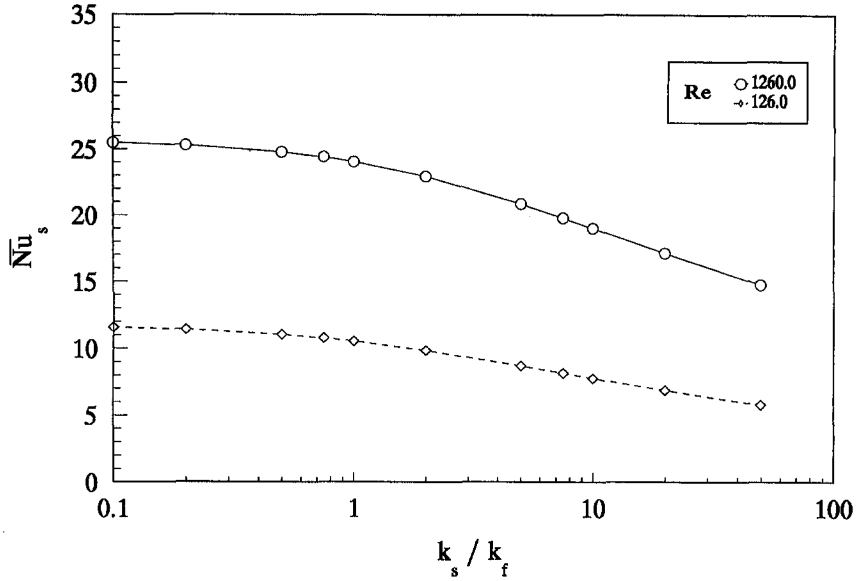

Fig. 7. Nusselt number averaged on the heat source varying with conductivity ratio for fully developed flow for the case of the insulated back-side of the board.

surface conductance will be included in a package thermal metric such as, θ_{j-a}, the junction to ambient thermal resistance. But if the surface conductance is dependent not only on the convective velocity field, but also on the upwind thermal boundary conditions that are due partly to upwind substrate conduction, the surface conductance cannot be specified *a priori*. Figure 7 demonstrates that the average Nusselt number on the source decreases with an increase in k_s/k_f by as much as a factor of two for low velocities. This decrease is due solely to conduction mechanisms, since the flow field is fully developed for all cases. The development of the flow field has an expected effect on the average source Nusselt number, as shown in Fig. 8, which presents the source averaged Nusselt number as a function of position of the source in the channel, with flow entering with a uniform velocity profile and maturing to a fully developed laminar channel flow. It is noteworthy that even with substrate conduction, *Nu* asymptotes to the constant value associated with fully developed hydrodynamics. The asymptotic fully developed flow values are indicated in Fig. 8.

Because of the utility of using the average surface heat transfer coefficient for practical calculations, we

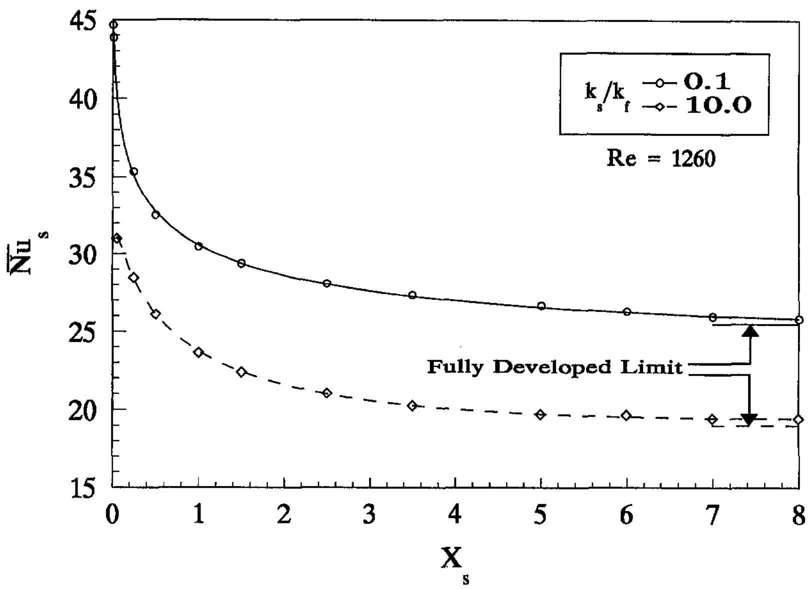

Fig. 8. Nusselt number averaged on the source varying with source position for laminar flow at Re = 1260.0 for the case of insulated back-side of the board.

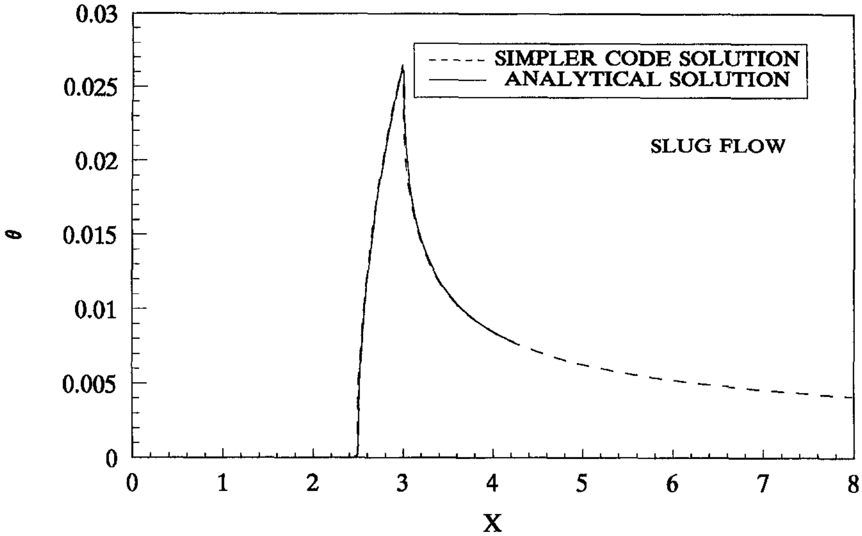

Fig. 9. Comparison of interface temperature for $k_s/k_f = 0.1$ for the case of insulated back-side of the board with the analytical solution for insulated substrate for slug flow at $Re = 1260.0$.

explore it a bit further. The spatial variation indicated in Fig. 8 is due to the development of the hydrodynamics from a uniform flow to a developed parabolic profile. The average heat transfer coefficient in the channel can thus be no greater than that from a uniform flow cooling the source, and no less than that from a fully developed flow cooling the source, regardless of substrate conduction effects. The reasons for this are readily apparent. In the absence of substrate conduction, this can be shown by existing analytic solutions For example, Fig. 9 depicts the comparison of the interface temperature for a near insulated substrate ($k_s/k_f = 0.1$) with an analytical solution available in Carslaw and Jaegar (reference [21], p. 269, equation (10)) for a strip source of heat on a perfectly insulated substrate cooled with uniform or slug flow. It can be observed that the present finite-volume SIMPLER-based solution is in very close agreement with the analytical solution. This agreement was found only with extremely fine meshing near the surface. The analytic solution for fully developed laminar channel flow may be found from an available solution for a step change in surface heat flux in a fully developed laminar channel flow, as presented for example in Shah and London (reference [22], p. 181, Table 34), for negligible streamwise heat diffusion. Again the present finite volume solution compares very well with the analytical solution, as shown in Fig. 10, for vanishingly small substrate conduction. A comparison of the two results is presented in a later section discussing the case of a convectively cooled back-side.

To this point, solutions have been presented for a single isolated source on a conducting substrate. The solution for a situation of multiple sources on a conducting substrate, interacting both convectively and conductively through the board, may be found by linear superposition of these single-source kernel solutions. The energy equations both on the solid side and the fluid side are linear with respect to temperature, thus allowing the superposition. This fact is verified numerically for two discrete identical flush-mounted constant powered heat sources embedded in a conductive substrate for the case where the back-side of the board is insulated. Figure 11 demonstrates the comparison between the superposed interface temperature solution and the actual temperature solution for two dicrete flush-mounted sources under fully developed flow conditions and k_s/k_f of 10.0. The length of the channel is 17 cm with the first source located at 5 cm from the inlet and the second source spaced 5 cm from the first source. Perfect agreement is observed as expected. It can be concluded that the solution for a single isolated source of heat on a conducting substrate may be used as a kernel solution thus reducing the computational time required for a thermal design tool.

The effects of upstream heating on the temperature of the convective flow over a source can be described in terms of a 'thermal wake', i.e. the board temperature downstream of the source. For the conjugate heat transfer problem, this temperature profile is dependent on both the board conduction and fluid convection in the vicinity of the source as previously shown. In the downstream region, the thermal wake is dependent only on the fluid convection and the total heat released by the source, therefore, the adiabatic board thermal wake models suggested in [18, 19] are applicable.

Back-side convectively cooled

We next consider the situation that arises when both sides of the board are convectively cooled. In Fig. 1, this corresponds to having a channel flow on the substrate back-side. For the present case, only the case for which the upper channel and the lower channel

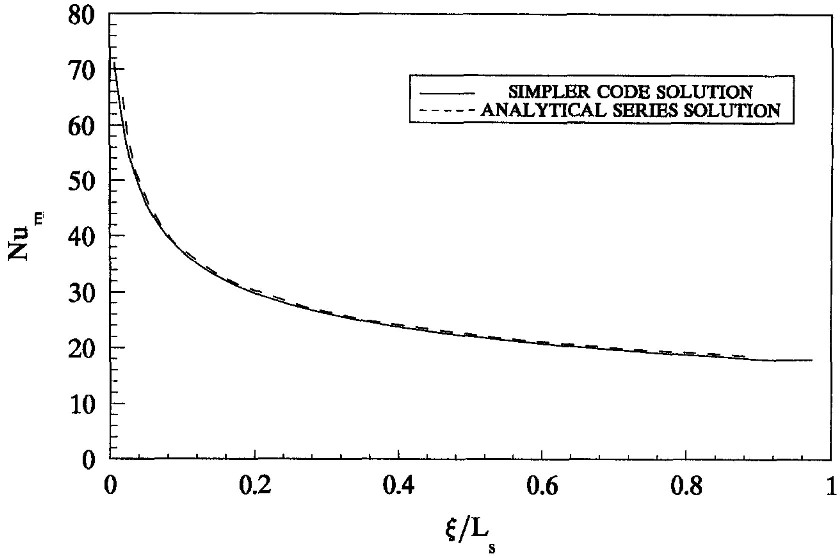

Fig. 10. Comparison of Nusselt number on the source for fully developed flow at $Re = 1260.0$ and $k_s/k_f = 0.1$ for the case of the insulated back-side of the board with an analytical solution for the insulated substrate.

were the same height was considered, thus, the flow develops similarly in both channels.

Figure 12 depicts the variation of heat flux from the board into the fluid on either side of the substrate. It shows the spreading of the heat flux by board conduction and decreasing peak values for higher values of k_s/k_f. It can be observed that there is a small negative heat flux downstream, indicating heat flow from the fluid into the board for $k_s/k_f = 1$. On the back-side, the peak heat flux occurs for $k_s/k_f = 10$, again emphasizing the competition between lateral heat spreading and penetration through the board. For the case of very high board conductivity the heat flux going into the fluid on both sides of the substrate is almost the same, for the reasons discussed previously. The heat flux variation is skewed as in the case of the insulated back-side because of lower convective resistance in the upstream region compared with that in the downstream region. An important observation that can be derived from these results is that an anisotropic board thermal conductivity may have significant effects on these results. The observed competition between normal as opposed to lateral conduction will be influenced by the difference in k_z compared with k_x and k_y. Frequently in multi-layer printed circuit boards, k_x and k_y are significantly increased due to signal and ground planes containing copper traces. Additional figures, which demonstrate the variation of the front-side and back-side temperatures and the Nusselt number for fully developed flow conditions and for board to fluid conductivity ratios varying between 0.1 and 100.0, may be found in the report of Sugavanam [15]. The Nusselt number averaged over the source is shown as a function of

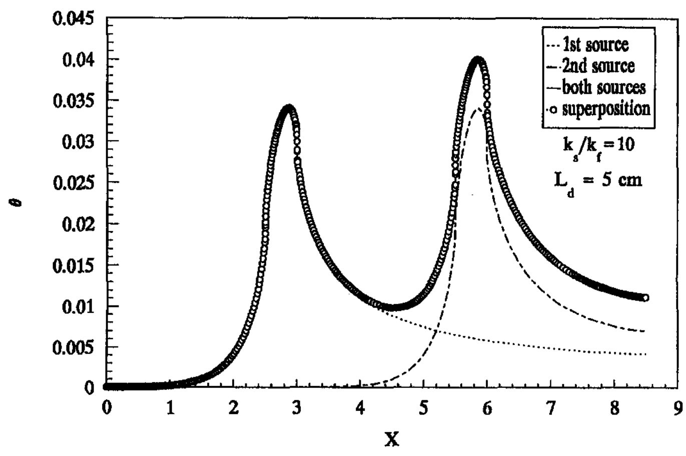

Fig. 11. Interface temperature varying with position for fully developed flow at $Re = 1260.0$ for two sources with $L_d = 5.0$ cm and $k_s/k_f = 10.0$ for the case of insulated back-side of the board.

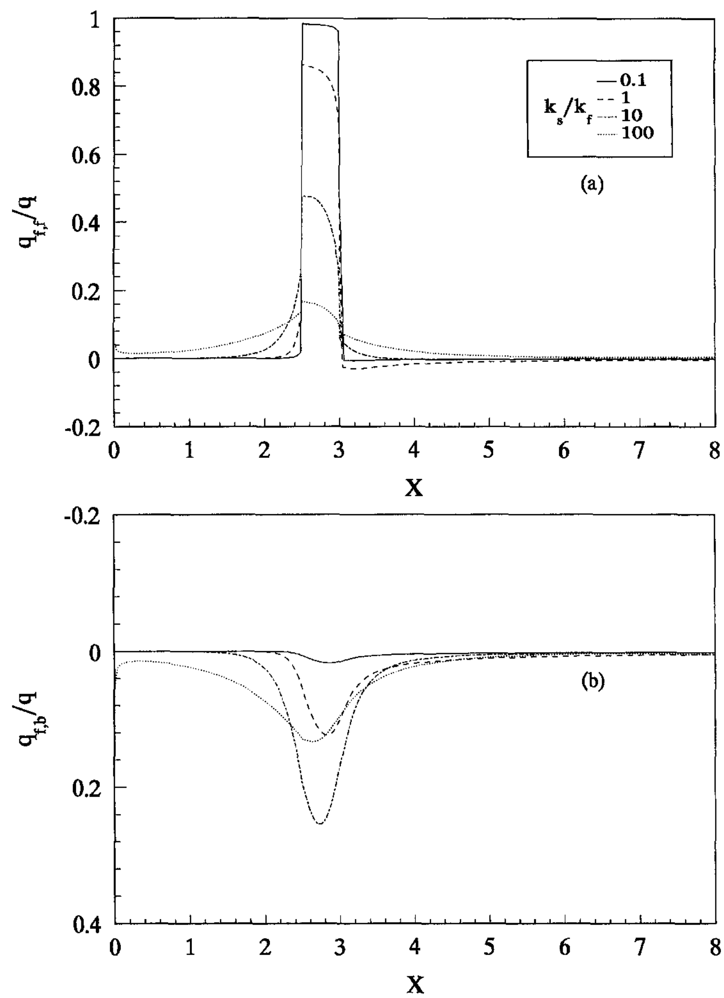

Fig. 12. Heat flux into the fluid on the (a) front-side and (b) back-side for fully developed flow at $Re = 1260.0$ for the case of the convectively cooled back-side of the board.

conductivity ratio for fully developed flow in Fig. 13. The variation of the source-average Nusselt number with the source position in the channel in a developing flow situation for a fixed Reynolds number is shown in Fig. 14. Figure 14 indicates that, as the source is moved far away from the entrance, the average Nusselt number approaches the value for the fully developed flow as expected. The average Nusselt number on the source for the source location near the entrance of the channel is still much lower than the Nusselt number corresponding to the previously mentioned case of uniform or slug flow conditions. This indicates that the maximum Nusselt number or cooling rate cannot exceed the slug flow limit for laminar flow situations. The slug flow and fully developed laminar flow limits on the source-averaged Nusselt number as a function of channel Reynolds number are shown in Fig. 15. The predictions are very similar to the case of the insulated back-side [15]. The values for the convectively cooled back-side are not very different from those for the case of an insulated back-side, for k_s/k_f of 0.1 and 1.0, indicating that the heat loss through the back-side for low substrate conductivities is very small. The diffusion limit is approached for both slug and fully developed flow as the Reynolds number approaches zero, and this serves as a consistency check for the code.

Substrate thickness variation

The effect of the variation of the thickness of the board on heat transfer characteristics was studied for fully developed conditions for both back-side-insulated and convectively cooled cases. In both cases, the calculated results showed only slight differences in the interface temperatures at low substrate conductivities, but at higher k_s/k_f, the temperature for a thicker substrate was much lower than that for the case of a thinner substrate [15]. Figure 16 shows the variation in the local Nusselt numbers for different substrate thicknesses and conductivities for the back-side convectively cooled cases. It was observed that the Nusselt numbers were not very different for low k_s/k_f values, but at high k_s/k_f values the Nusselt numbers varied with different substrate thicknesses. Nevertheless, this

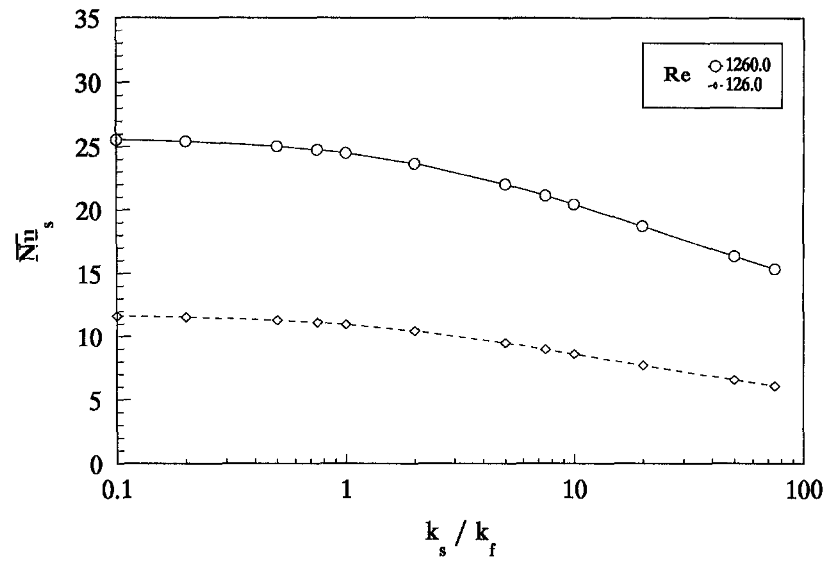

Fig. 13. Average Nusselt number on the source varying with conductivity ratio for fully developed flow for the case of convectively cooled back-side of the board.

difference was less than 10% even in the case of k_s/k_f of 100.0.

Correlations

An effort was made to collapse the data for the average Nusselt number on the source varying with Peclet number and the conductivity ratio for hydrodynamically fully developed flow conditions. The variation for $\overline{Nu}_s$ was assumed as follows:

$$\frac{\overline{Nu}_s}{\overline{Nu}_{s(ad)}} = f\left(\frac{k_s}{k_f}, Pe\right) \tag{20}$$

where $\overline{Nu}_{s(ad)}$ is the Nusselt number for the adiabatic case ($k_s/k_f = 0$). The function was forced to yield to unity when k_s/k_f reduced to zero. After a series of trials, the following correlation was chosen.

$$\frac{\overline{Nu}_s}{\overline{Nu}_{s(ad)}} = (1.186Pe^{-0.013})^{-(k_s/k_f)0.586}. \tag{21}$$

The above correlation compared with the actual solution within 1.2% for $0 \leqslant k_s/k_f \leqslant 10$. Alternatively, a simpler form valid for $0.1 \leqslant k_s/k_f \leqslant 10.0$ can be stated as

$$\overline{Nu}_s = 1.833(Pe)^{0.37}\left(\frac{k_s}{k_f}\right)^{-0.0754}. \tag{22}$$

The correlation compared with the actual solution to within 10%.

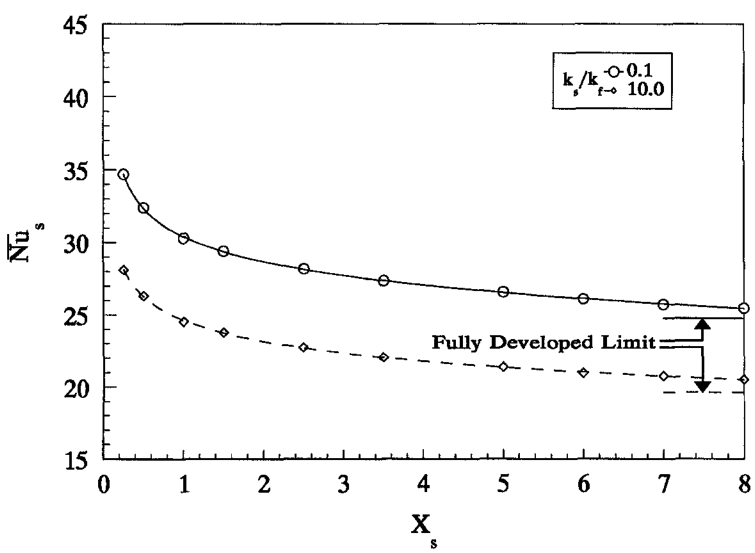

Fig. 14. Nusselt number averaged on the source varying with source position for laminar flow at $Re = 1260.0$ for the case of the convectively cooled back-side of the board.

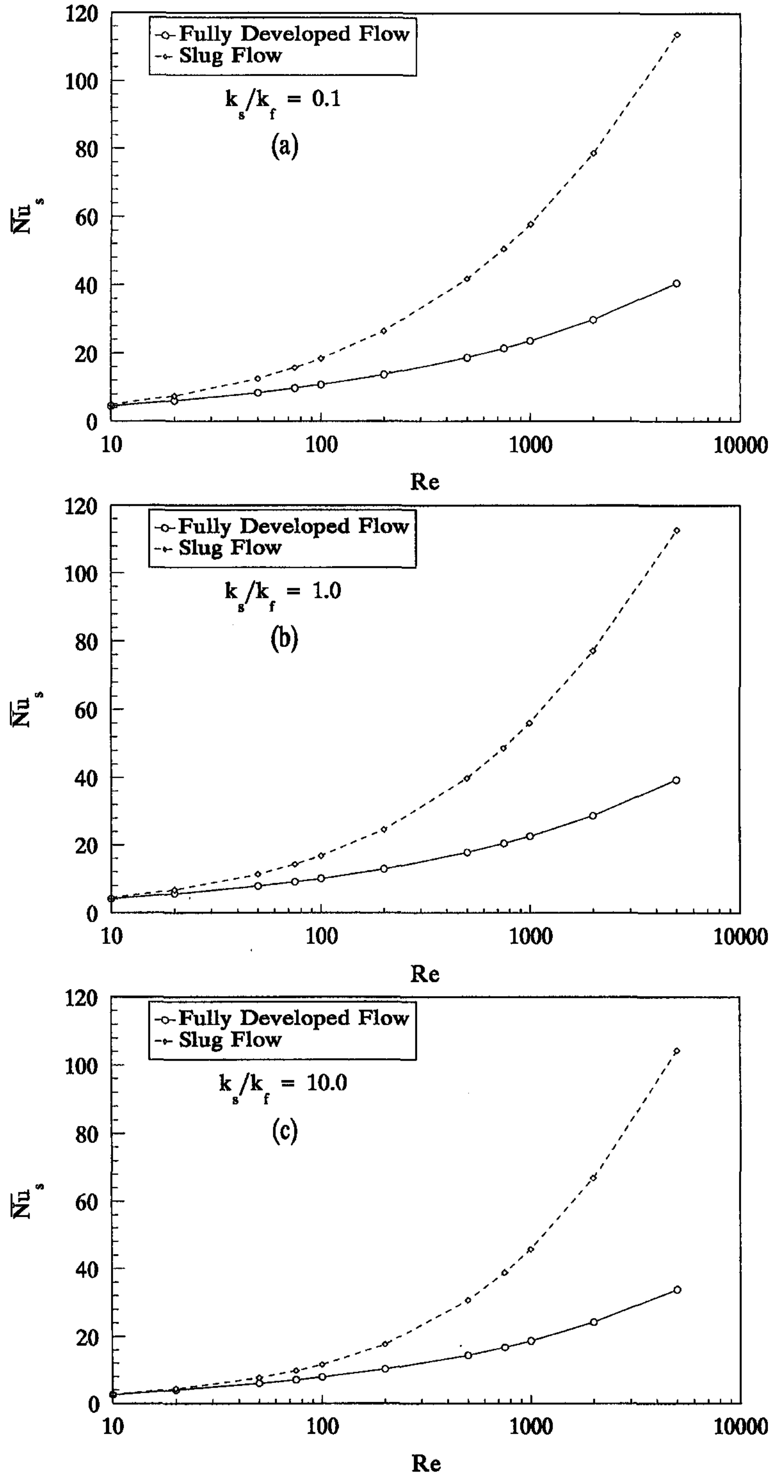

Fig. 15. Average Nusselt number on the source for fully developed flow and slug flow varying with Reynolds number for the case of convectively cooled back-side of the board.

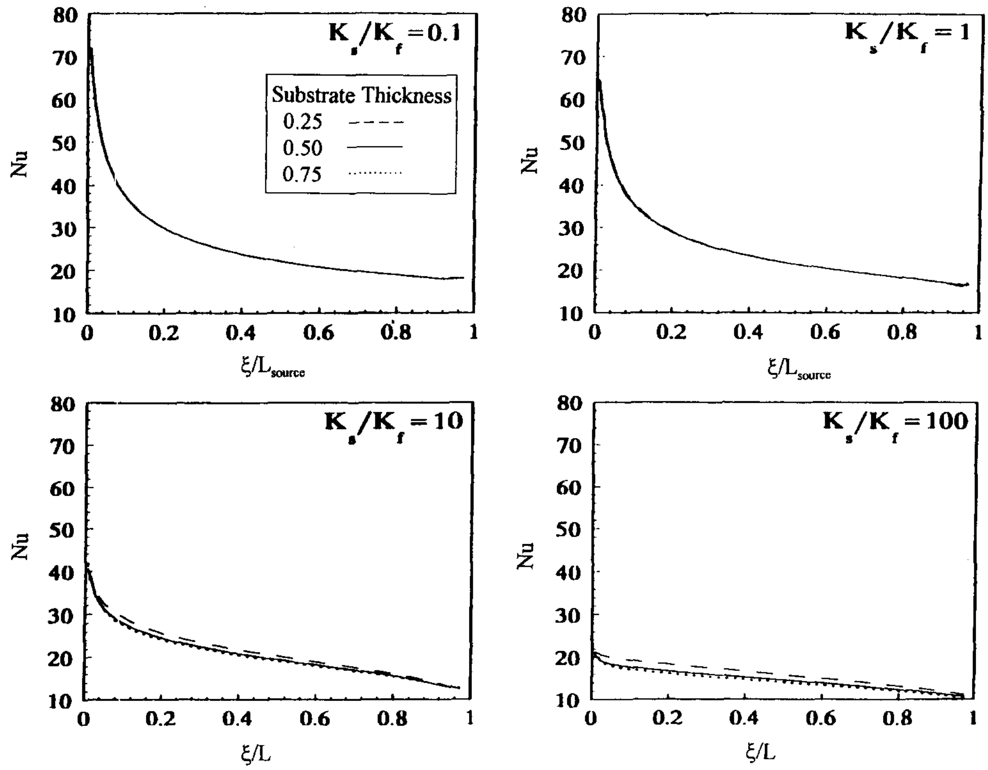

Fig. 16. Comparison of Nusselt numbers on the source for substrate thicknesses at 0.25, 0.5 and 0.75 cm for fully developed flow at $Re = 1260.0$ for the case of convectively cooled back-side of the board.

CONCLUSIONS

Conjugate heat transfer from thin flush-mounted heat sources in parallel-plate channels for forced laminar convection was investigated in this study. Efforts were focused on examining the heat transfer in a conjugate-coupled sense. Numerical solutions were obtained for flow conditions varying from slug flow to hydrodynamically fully developed flow and conductivity ratios varying from 0.1 to 100. Results from this study were found to be consistent with available analytical solutions for special cases. The heat transfer behavior for a wide range of parameters has been clearly demonstrated. The far-field wake temperatures merged for all the substrate conductivities for the case of an insulated back-side. For any developing flow domain, the Nusselt number was forced to be bounded by the slug flow limit and the fully developed flow limit at a given Reynolds number. Preheating by board conduction increased at higher k_s/k_f values and thereby decreased the Nusselt number upstream of the source and on the source. The Nusselt number for the slug flow situation was found to be much higher when compared with that of the fully developed flow situation at high Reynolds numbers because of convection predominance. The effects of substrate thickness were important only for conductivity ratio, $k_s/k_f > 10$. The validity of the superposition principle to predict temperatures on the board for multiple heat sources was demonstrated.

Acknowledgements—This work was supported in part by a grant from the IBM Corporation through the Shared University Research Program (SUR), and in part by the National Science Foundation through a PYI grant, grant no. CTS-9057465, to the senior author. We gratefully acknowledge the support and advice of Dr Sung Jin Kim of IBM-Tucson.

REFERENCES

1. G. P. Peterson and A. Ortega, Thermal control of electronic equipment and devices, *Adv. Heat Transfer* **20**, 181–314 (1990).
2. E. Baker, Liquid cooling of microelectronic devices by free and forced convection, *Microelectron. Reliability* **11**, 213–222 (1972).
3. A. Brosh, D. Degani and S. Zalmanovich, Conjugated heat transfer in a laminar boundary layer with heat source at the wall, *ASME J. Heat Transfer* **11**, 709–724 (1992).
4. S. Ramadhyani, D. F. Moffatt and P. F. Incropera, Conjugate heat transfer from small isothermal heat sources embedded in a large substrate, *Int. J. Heat Mass Transfer* **28**, 1945–1952 (1985).
5. F. P. Incropera, J. S. Kerby, D. F. Moffat and S. Ramadhyani, Convection heat transfer from discrete heat sources in a rectangular channel, *Int. J. Heat Mass Transfer* **29**, 1051–1058 (1986).
6. J. R. Culham, T. F. Lemcyzk, S. Lee and M. M. Yovanovich, META—a conjugate heat transfer model for air cooling of circuit boards with arbitrarily located heat sources, *ASME Heat Transfer in Electronic Equipment* **HTD-171**, 117–126 (1991).
7. J. R. Culham and M. M. Yovanovich, The effect of common design parameters on the thermal performance

of microelectronic equipment: Part II—forced convection, *ASME Heat Transfer in Electronic Equipment* **HTD-171**, 55–62 (1991).
8. J. Davalath and Y. Bayazitoglu, Forced convection cooling across rectangular blocks, *ASME J. Heat Transfer* **109**, 321–328 (1987).
9. S. H. Kim and N. K. Anand, Laminar developing flow and heat transfer between a series of parallel plates with surface mounted discrete heat sources, *Int. J. Heat Mass Transfer* **37**, 2231–2244 (1994).
10. S. H. Kim and N. K. Anand, Turbulent heat transfer between a series of parallel plates with surface-mounted discrete heat sources, *ASME J. Heat Transfer* **116**, 577–587 (1994).
11. C. Y. Choi, S. K. Kim and A. Ortega, Effects of substrate conductivity on convective cooling of electronic components, *ASME J. Electronic Packaging* **116**, 198–205 (1994).
12. J. S. Nigen and C. H. Amon, Time-dependent characteristics of conjugate heat transfer characteristics of self-sustained oscillatory flows in a grooved channel, *ASME J. Fluids Engng* (1994).
13. A. Ortega, U. Wirth and S. J. Kim, Conjugate forced convection from a discrete heat source on a plane conducting surface: a benchmark experiment, *ASME Heat Transfer in Electronic Systems*, **HTD-292**, 25–36 (1994).
14. S. V. Patankar, *Numerical Heat Transfer and Fluid Flow*. Hemisphere, New York (1980).
15. R. Sugavanam, Numerical investigation of conjugate heat transfer from flush heat sources on a conductive board in laminar channel flow, M.S. Thesis, The University of Arizona, Tucson, AZ (1994).
16. G. de Vahl Davis and I. P. Jones, Natural convection of air in a square cavity: A benchmark numerical solution, *Int. J. Numer. Methods Fluids* **3**, 249–264 (1983).
17. F. M. White, *Viscous Fluid Flow* (2nd Edn). McGraw-Hill, New York (1991).
18. A. Ortega, S. Ramanathan, J. D. Chicci and J. L. Prince, Thermal wake models for forced air cooling of electronic components, *Proc. Semitherm IX, IEEE* 93*CH*3226-8, pp. 63–74 (1993).
19. S. Ramanathan and A. Ortega, A uniform flow effective diffusivity model for forced air cooling of electronic components, *ASME J. Heat Transfer* (in review, 1995).
20. A. Zebib and Y. K. Wo, A two dimensional conjugate heat transfer model for forced air cooling of an electronic device, *ASME J. Electronic Packaging* **9**, 11–16 (1989).
21. H. S. Carslaw and J. C. Jaegar, *Conduction of Heat in Solids* (2nd Edn), p. 269. Clarendon Press, Oxford (1959).
22. R. K. Shah and A. L. London, Laminar flow forced convection in ducts, *Advances in Heat Transfer*. Academic Press, New York (1978).